Journal of Theoretical Biology 420 (2017) 105–116

Contents lists available at ScienceDirect

Journal of Theoretical Biology

journal homepage: www.elsevier.com/locate/yjtbi

A simple model of cardiac muscle for multiscale simulation: Passive mechanics, crossbridge kinetics and calcium regulation☆

Fyodor A. Syomin[a,b], Andrey K. Tsaturyan[a,b,*]

[a] Department of Biomechanics, Institute of Mechanics, Moscow University, 1 Mitchurinsky prosp., Moscow 119192, Russia
[b] Eltsyn Ural Federal University, 19 Mira Str., Ekaterinburg 620002, Russia

ARTICLE INFO

Keywords:
Cardiac muscle
Modeling
Actin-myosin interaction
Ca-activation
Contraction
Relaxation

ABSTRACT

A simple model of cardiac muscle was designed for multiscale simulation of heart mechanics. Relaxed cardiac muscle was described as a transversally isotropic hyperelastic material. Active tension caused by actin-myosin crossbridges depends on the ensemble averaged strain of myosin heads bound to actin. Calcium activation was modeled by Ca^{2+} binding to troponin-C. To account for the dependence of troponin affinity for Ca^{2+} on myosin heads strongly bound to actin, the kinetics of troponin binding to Ca^{2+} in the overlap zone of the thin and thick filaments and outside it were separated. The changes in the length of these zones during muscle shortening or lengthening were accounted for explicitly. Simplified version of the model contains only 5 ordinary differential equations (ODE). Model parameters were estimated from a limited set of experiments with skeletal and cardiac muscle. Simulations have shown that model reproduces qualitatively a number of experimental observations: steady-state force-velocity and stiffness-velocity relations; mechanical responses to step changes in muscle length or load; steep Ca^{2+}-tension relationship and its dependence on sarcomere length tension (the Frank-Starling mechanism); tension, shortening and Ca^{2+}-transients in twitch isometric and isotonic contractions, tension development and redevelopment upon fast change in Ca^{2+} concentration or muscle release followed by re-stretch. We believe that the model can be effectively used for modeling contraction and relaxation of the heart.

1. Introduction

Simulation of the pumping function of the heart requires a model that describes mechanical properties of cardiac muscle during passive stretch, contraction and relaxation. Such model should incorporate macroscopic constitutive stress-strain relationship and its dependence on molecular events including actin-myosin interaction and its regulation by Ca^{2+} ions via troponin (Tn) and tropomyosin (Tpm). The model should reproduce all main properties of cardiac muscle observed in experiments with single cells or small tissue samples. On the other hand, the model should be simple computationally to enable simulation of 3D contraction of the left ventricle or all heart chambers. This means that the material model should be described by a system of ODE, not by partial differential equations like it was done in the first kinetic model of muscle contraction (Huxley, 1957) and its modern versions such as (Smith et al., 2008). The ODE system should not be 'stiff' to allow one to use rather large time steps of a solver. A number of models of myocardial mechanics and regulation have been suggested in last twenty five years (Izakov et al., 1991; Hunter et al., 1998; Razumova et al., 1999, 2000) including several recent and most advanced ones (Niederer et al., 2006; Rice et al., 2008; Markhasin et al., 2003; see also review by Trayanova and Rice, 2011). These models describe actin-myosin crossbridges and Ca^{2+} regulation (in some cases together with cardiac electrophysiology) by a system of ODEs. However there is no 'standard' model, which completely satisfies all criteria listed above. Some models contain too many differential equations or ODE system is too stiff and requires too small time steps for computer integration to be effectively used in 3D simulations; the others do not reproduce some basic important features of contraction, relaxation or regulation.

Here we present a simple model that was designed to fill the gap between the 'overcomplicated' and 'oversimplified' models of cardiac muscle. It was designed to reproduce the following set of experimental data.

1. Steady-state force-velocity and stiffness-velocity relationships at full and incomplete activation during shortening (Hill, 1938; Julian Morgan, 1981; Ford et al., 1985) and lengthening (Lombardi and

☆ The authors have no conflict of interest to declare regarding publication of this paper.

* Correspondence to: Institute of Mechanics, Moscow University, Moscow 119192 Russia.
E-mail address: tsat@imec.msu.ru (A.K. Tsaturyan).

http://dx.doi.org/10.1016/j.jtbi.2017.02.021
Received 29 August 2016; Received in revised form 9 February 2017; Accepted 16 February 2017
Available online 20 February 2017

Piazzesi, 1990) of skeletal or cardiac (Chiu et al., 1987) muscles.
2. Mechanical transients induced by step changes in length or load at full and partial activation of skeletal (Civan and Podolsky, 1966; Ford et al., 1977, 1985, 1986; Piazzesi et al., 1992, 2002) or cardiac (Chiu et al., 1982; Colomo et al., 1994) muscles.
3. Tension responses to ramp stretches of different velocity (Lombardi and Piazzesi, 1990).
4. Frequency dependencies of the elastic and viscous moduli observed in tension response to small-amplitude oscillations of muscle length (Kawai et al., 1981; Saeki et al., 1991).
5. Steep Ca-force relationship even in the absence of myosin heads and it modulation by actin-bound myosin heads (Sun et al., 2009; Sun and Irving, 2010).
6. Increase in Tn affinity for Ca^{2+} Tn upon binding of myosin heads to actin (Martyn and Gordon, 2001).
7. Length-dependent activation, i.e., the dependence of the Ca-force relation on sarcomere length (Dobesh et al., 2002; de Tombe et al., 2010).
8. Tension responses of single cardiac myofibrils to the fast increase in Ca^{2+} concentration and tension redevelopment after mechanical perturbation (Piroddi et al., 2007).
9. Load-dependent relaxation, i.e., acceleration of relaxation of cardiac muscle after shortening during isotonic contraction (Parikh et al., 1993).

On the other hand, we tried to reduce the number of ODE and the number of the model parameters paying particular attention to computational simplicity of the model. The latter means that we tried to eliminate "fast variables" which lead to "stiffening" of an ODE system. An earlier version of the model (Syomin and Tsaturyan, 2012; Syomin, 2014) was essentially modified and simplified here.

As the experiments listed above were performed on different muscles from different species we did not try to fit them all quantitatively with a single set of parameter. Instead we tried to use dimensionless variables and parameters to facilitate model tuning for a particular type of muscle from particular specie. When possible we tried to reproduce the characteristics of cardiac muscle from human ventricle. Currently our model is rather qualitative or semi-quantitative than quantitative. We, however, believe its parameters can be adjusted to describe properties of ventricular tissue from particular species.

2. Material and methods: model description

All model variables and parameter values are listed in Table 1.

2.1. Constitutive equation

We consider cardiac muscle as an anisotropic incompressible continuous medium. Passive stress is assumed to be hyperelastic, while active stress is postulated to be quasi-one-dimensional, as it was suggested and experimentally verified for skeletal muscle (Bershitsky and Tsaturyan, 1981). The Cauchy stress tensor $\hat{T}$ is described by the expression:

$$\hat{T} = \left(\frac{\partial\Phi(I_1, I_2)}{\partial I_1} + I_1\frac{\partial\Phi(I_1, I_2)}{\partial I_2}\right)\hat{F} - \frac{\partial\Phi(I_1, I_2)}{\partial I_2}\hat{F}^2 - p\hat{E} + \hat{B}(T_{tit} + T_A), \quad (1)$$

where Φ is the isotropic strain energy density which depends on the first two invariants of the left Cauchy–Green deformation strain tensor $\hat{F}$, I_1, I_2. The third invariant of $\hat{F}$, $I_3 \equiv 1$ due to incompressibility; $\hat{E}$ is the unit tensor, p is the Lagrange factor caused by incompressibility, T_{tit} is a scalar that describes the anisotropic passive tension of intra-sarcomere cytoskeleton mainly caused by titin filaments; T_A is active tension produced by the actin-myosin interaction. $\hat{B} = \vec{l} \otimes \vec{l}$ is the anisotropy tensor is equal to the tensor square of the unit vector $\vec{l}$ aligned with the direction of muscle fibres in deformed muscle. The

Table 1
Model variables and parameters.

Variable or parameter	Meaning	Value
$\hat{T}$	Cauchy stress tensor	
$\hat{F}$, $\hat{G}$	Finger and right Cauchy-Green strain tensors	
Φ	Density of isotropic elastic energy	
I_1, I_2, I_3	Invariants of $\hat{F}$	
$\hat{E}$	Unit tensor	
$\hat{B}$	Tensor of transversal anisotropy	
$\vec{l}$, $\vec{l}_0$	Unit vector aligned with muscle fibres ($\vec{l}_0$ is $\vec{l}$ in undeformed state)	
T_{tit}	Titin tension	
T_A, T_A^0	Active tension and its value at full activation and full filament overlap	
a_0, kN/m^2	Constant parameter	0.55
a_1	Constant parameter	3
l_s, μm	Sarcomere length	
l_{s0}, μm	Reference sarcomere length	1.9
E, pN/nm	Crossbridge stiffness	2.5
e, nm	Effective compliance of actin and myosin filaments	2
N_M, 10^{14}/m^2	Number of myosin filaments per unit cross-section area	2.5
N_{xb}	The number of myosin heads per a half of a thick filament	150
k_B, 10^{-23} J/K	Boltzmann constant	1.38
T, K	Absolute temperature	310
P, nm	Persistence length of titin molecule	0.5
L, nm	Contour length of titin in sarcomere	800
n, n_1, n_2	Fractions of myosin heads attached to actin (total, and in states 1 and 2, respectively)	
A_1, A_2	Fractions of troponin complexes in the C- and O-states filament overlap zone and outside it, respectively	
f_+, f_-, g, H_+, H_-	Rates of transitions between crossbridge states 0→1, 1→0, 2→0, 1→2 and 2→1, respectively	
δ, δ_1, δ_2, nm	Ensemble averaged crossbridge distortion (total and in states 1 and 2, respectively)	
h, nm	Axial displacement of a crossbridge during transition from state 1 to state 2 at zero load	10
$W(l_s)$, nm	Length of overlap zone as function of sarcomere length	
$\delta' = \delta/h$	Dimensionless δ	
$f_+^0 = f_+(0)$, s^{-1}		75
$\varepsilon = f_+^0/H_-$	Ration of rate constants	0.05
$F(\delta)$, $G(\delta)$	Dimensionless rates of crossbridge binding and unbinding	
γ	Constant parameter	4
$\theta = n_2/n$	Fraction of force generating crossbridges	
δ_*	Upper limit for δ during stretch	0.4
b	Constant parameter	1.5
c	Constant parameter	8.5
α_+, s^{-1}	Rate constant of Ca^{2+} binding to Tn	35
k_s	Constant parameter	2
k_n	Constant parameter	8
C_0, μM	Ca^{2+} concentration half-saturating Tn at l_{s0} in the absence of myosin heads	2
C_{Tn}, μM	Total concentration of Tn	70
B	Normalized concentration of Ca^{2+} buffer in cytoplasm (different from Tn)	50
K_B	Normalized equilibrium constant of cytoplasm Ca^{2+} buffer	0.5
λ, s^{-1}	Rate constant of Ca^{2+} uptake into sarcoplasmic reticulum	500
m	Hill parameter	3
K_i	Normalized inhibitory constant of Ca2+ uptake to SR	2
$a(l_s, n\theta)$	Dimensionless rate of Ca^{2+} release from Tn	
k_1, s^{-1}	Rate constant of accelerated Ca^{2+} release	15
k_2, s^{-1}	Rate constant of deceleration of Ca^{2+} release	200
Q^*, s^{-1*}	Maximal rate of Ca^{2+} release from SR	700
c_*	Normalized Ca^{2+} concentration at rest	0.05
l_a, μm	Length of an actin filament	1.1

isotropic elastic potential Φ was taken in the form similar to that of (Guccione et al., 1991):

$$\Phi = a_0 exp(a_1((I_1-3)^2-2(I_2-2I_1+3))), \quad (2)$$

where a_0, a_1 are constant parameters.

Sarcomere length l_s can be determined as follows (Lurie, 1990):

$$l_s = l_{s0}\sqrt{\vec{l}_0\hat{G}\vec{l}_0}, \quad (3)$$

where l_{s0} is the reference sarcomere length, i.e., sarcomere length in unloaded passive myocardium, and $\hat{G}$ is the right Cauchy-Green deformation tensor, $\vec{l}_0$ is unit vector aligned with fibres in unstrained muscle.

During stretch, T_{tit} is mainly determined by titin filaments while upon compression it is governed by the resistance of the thick filaments and other structures as follows:

$$T_{tit} = \begin{cases} N_M \frac{6k_BT}{P}\left(\frac{1}{4}(1-\frac{l_s-l_{s0}}{L})^{-2} + \frac{l_s-l_{s0}}{L} - \frac{1}{4}\right), & l_s \geq l_{s0}, \\ N_M \frac{9k_BT}{PL}(l_s - l_{s0}), & l_s < l_{s0}, \end{cases} \quad (4)$$

where N_M is the number of the myosin filaments per unit cross-section area of muscle in its initial reference state; expression in brackets in the upper formula was suggested by Marko and Siggia (1995) for approximation of the force caused by stretch of a worm like chain; L is the total, or 'contour', length of titin; P is so called persistence length, k_B and T are the Boltzmann constant and absolute temperature. Factor 6 arises from the fact that there are six titin molecules which connect each half of a myosin filament to a Z-disk (Liversage et al., 2001). At sarcomere length below l_{s0} passive sarcomeric tension is assumed to be Hookean. Our model of passive mechanics of cardiac muscle has four parameters as widely accepted model of Guccione *et al.* does (Guccione et al., 1991). It, however, is simpler because muscle anisotropy in our model is essentially one-dimensional and fully attributed to titin filaments which are aligned with muscle fibres. Mechanical properties of titin are well described by a worm-like chain model on a single molecular level (Leake et al., 2004).

2.2. Crossbridge kinetics

We used a kinetic scheme of the actin-myosin interaction based on the Lymn-Taylor cycle (1971) similar to that of Razumova et al. (1999). Just after binding to actin, a myosin head is in a pre-force-generating state 1 and then it can either detach or undergo a transition to force-generating state 2. The transition is associated with a tilt of myosin head that is equivalent to displacement (filament sliding) of a distance h. Following H.E. Huxley and A.F. Huxley we use term 'crossbridges' for actin-bound myosin heads. Active tension is given by an expression:

$$T_A = EN_MN_{xb}W(l_s)(\delta_1 n_1 + n_2(h+\delta_2)),$$

where N_{xb} is the total number of myosin heads per a half of a myosin filament; $W(l_s)$ is the length of the overlap zone of the thick and thin filaments in a half-sarcomere normalized by its maximal value; E is constant crossbridge stiffness, n_1 and n_2 are the probabilities of being in the states 1 and 2 respectively for a myosin head in the filament overlap zone of a sarcomere. The probability for a head to be in detached state is 1 - n_1 - n_2. Here δ_1 and δ_2 are the ensemble average distortions of the crossbridges in states 1 and 2, respectively. These values are similar to values x_1 and x_2 used in model of Razumova et al. (1999) with the only difference that x_2 in their model corresponds to δ_2+hin our model. The kinetic equations for n_1, n_2 are as follows:

$$\begin{aligned} \frac{\partial n_1}{\partial t} &= f_+(A_1 - n_1 - n_2) - f_- n_1 - H_+ n_1 + H_- n_2, \\ \frac{\partial n_2}{\partial t} &= -gn_2 + H_+ n_1 - H_- n_2. \end{aligned} \quad (5)$$

Here f_+, f_-, H_+, H_-, g are the rate constants. A_1 the degree of the muscle activation, i.e., the availability of actin site for myosin heads. Its meaning is specified below. We used the main idea of Thorson and White (1983), i.e., an assumption that all five rates f_+, f_-, h_+, h_-, g depend only on the average strains, or the ensemble averaged, cross-bridge distortions, δ_1 and δ_2.

The equations which describe the kinetics of the total average strain of all crossbridges in states 1 and 2 can be written as:

$$\begin{aligned} \frac{\partial(n_1\delta_1)}{\partial t} &= \frac{n_1}{2}\left(\frac{\partial l_s}{\partial t} - \frac{2e}{T_A^0}\frac{\partial T_A}{\partial t}\right) - f_- n_1\delta_1 - H_+ n_1\delta_1 + H_- n_2\delta_2, \\ \frac{\partial(n_2\delta_2)}{\partial t} &= \frac{n_2}{2}\left(\frac{\partial l_s}{\partial t} - \frac{2e}{T_A^0}\frac{\partial T_A}{\partial t}\right) - gn_2\delta_2 + H_+ n_1\delta_1 - H_- n_2\delta_2. \end{aligned} \quad (6)$$

Here e is a parameter (assumed to be constant) that characterizes the compliance of the thick and thin filaments in a sarcomere and T_A^0 is T_A during steady-state isometric contraction at full activation, i.e., at A_1=1. In contrast to the model of Razumova et al. (1999) where H_+, H_- were small compared to f_+, f_-, g we use the idea of Huxley and Simmons (1971) that was confirmed by time-resolved x-ray diffraction data (Lombardi et al., 1995) that the force-generation transition and its reversal are much faster than crossbridge detachment and attachment, i.e., $H_+, H_- \gg f_+, f_-, g$. The Eq. (5) are the same as those in the model of Razumova et al. (1999), while in Eq. (6) they omitted the terms which describe the change in the crossbridge distortion due to the transitions between states 1 and 2.

Using Eq. (5), one can rewrite Eq. (6) as follows

$$n_1\frac{\partial\delta_1}{\partial t} = \frac{n_1}{2}\left(\frac{\partial l_s}{\partial t} - \frac{2e}{T_A^0}\frac{\partial T_A}{\partial t}\right) - f_+(A_1 - n_1 - n_2)\delta_1 + H_-n_2(\delta_2 - \delta_1),$$

$$n_2\frac{\partial\delta_2}{\partial t} = \frac{n_2}{2}\left(\frac{\partial l_s}{\partial t} - \frac{2e}{T_A^0}\frac{\partial T_A}{\partial t}\right) + H_+n_1(\delta_2 - \delta_1).$$

The difference between δ_1 and δ_2 obeys an equation:

$$\frac{\partial(\delta_2 - \delta_1)}{\partial t} = \frac{(A_1 - n_1 - n_2)}{n_1}f_+\delta_1 - \left(H_-\frac{n_2}{n_1} + H_+\frac{n_1}{n_2}\right)(\delta_2 - \delta_1).$$

Therefore, if $H_+, H_- \gg f_+, f_-, g$ and n_1 is not very small, one can neglect the difference between δ_1 and δ_2 to use the approximation $\delta_1 = \delta_2 = \delta$ as this was done in our earlier paper (Syomin and Tsaturyan, 2012). In this case the crossbridge kinetics is described by two Eq. (5) and equation for δ in the form:

$$\frac{\partial\delta}{\partial t} = \frac{1}{2}\frac{\partial l_s}{\partial t} - \frac{e}{T_A^0}\frac{\partial T_A}{\partial t} - \frac{(A_1 - n)}{n}f_+\delta, \quad (7)$$

where $n = n_1 + n_2$.

We have shown previously that a model of this kind is able to describe many principal steady and non-steady experiments with skeletal muscle fibres at full activation and full overlap between the thin and thick filaments. In particular, that model explained nonlinear partial tension recovery after step length changes applied during isometric contraction (Ford et al., 1977), during steady shortening (Ford et al., 1985) or lengthening (Piazzesi et al., 1992) as well as length responses to step change in load (Piazzesi et al., 2002).

Further simplification of the model that, importantly, leads to a decrease in "stiffness" of the ODE system can be achieved if one excludes from consideration very fast processes which take place during the first two milliseconds after a length or force step change. Following (Huxley and Simmons, 1971) and our earlier work (Syomin and Tsaturyan, 2012) we assume that $H_-=const$. We introduce dimensionless distortion $\delta' = \delta/h$ and additionally assume that at $\delta'<0$, $f_+(\delta) = f_+^0 = const$ (Syomin and Tsaturyan, 2012). Using these constants we introduce dimensionless time $t' = f_+^0 t$. Then the dimensionless rate constants can be written in the form: $H_- = f_+^0/\varepsilon$, where $\varepsilon \ll 1$.

Following (Huxley and Simmons, 1971) we set $H_+ = \frac{f_+^0 \exp(-\gamma\delta)}{\varepsilon}$, where α is a constant. We then change for dimensionless variables and omit prime in time and distortion every time when this cannot cause any ambiguities. We introduce new variable $\theta=n_2/n$ and rewrite (5) and (7) in the form

$$\frac{\partial\delta}{\partial t} = \frac{1}{2h}\frac{\partial l_s}{\partial t} - \frac{e}{h}\frac{\partial T_A}{\partial t} - \delta F\frac{(A_1 - n)}{n},$$
$$\frac{\partial n}{\partial t} = F(\delta)(A_1 - n) - n(G_-(\delta)\theta(t) + F_-(\delta)(1-\theta(t))), \quad (8)$$
$$\varepsilon\frac{\partial\theta}{\partial t} = \frac{\theta_0(\delta) - \theta}{1 + \exp(-\gamma\delta)} - \varepsilon\theta\left(\frac{F_+(\delta)(A_1 - n)}{n} - (G_-(\delta)\theta(t) + F_-(\delta)(1-\theta(t)))\right)$$

where $F(\delta) = \frac{f_+(\delta)}{f_+^0}$, $F_-(\delta) = \frac{f_-(\delta)}{f_+^0}$, $G_+(\delta) = \frac{g(\delta)}{f_+^0}$ and $\theta_0(\delta) = \frac{\exp(-\gamma\delta)}{1+\exp(-\gamma\delta)}$.

After omitting the last term in the last equation of (8) and applying to this equation the method of the inner and outer expansions, we obtained an equation for $\theta(t)$ that is correct within the accuracy up to the terms of the first order of ε:

$$\theta(t) = (\theta(t_0) - \theta_0(\delta))\exp\left(-\frac{t - t_0}{\varepsilon(1 + \exp(-\gamma\delta))}\right).$$

The method the inner and outer expansions is based on the separation of two time scales: the 'fast' dimensionless time t/ε and the slow dimensionless time t. If $\varepsilon \ll 1$, one can 'freeze' the slow time t and solve the equation for the θ as function of the fast time only. A useful notation for the total dimensionless crossbridge detachment rate is:

$$G(\delta) = G_-\theta_0(\delta) + F_-(1-\theta_0(\delta)).$$

We therefore can rewrite (8) in a simplified form as

$$\frac{\partial\delta}{\partial t} = \frac{1}{2h}\frac{\partial l_s}{\partial t} - \frac{e}{h}\frac{\partial T_A}{\partial t} - \delta F\frac{(A_1 - n)}{n}, \quad \frac{\partial n}{\partial t} = F(\delta)(A_1 - n) - nG(\delta), \quad (8')$$
$$\theta(t) = (\theta(t_0) - \theta_0(\delta))\exp\left(-\frac{t - t_0}{\varepsilon(1 + \exp(-\gamma\delta))}\right) + \theta_0(\delta),$$

that is particularly useful for computational purposes as one can use a relatively large time step of order of $1/f_+^0$ for first two equations while the fast components of changes in variables can be calculated using an approximate formula. For relatively slow processes lasting more than 2–3 ms one can assume that $\theta(t) = \theta_0(\delta)$ and omit the term that contains filament compliance e in the 1st equation in Eq. (8′)

Functions F and G were set as follows:

$$F(\delta) = \begin{cases} 1, & \delta \le 0, \\ \frac{\delta_*^2}{(\delta_* - \delta)^2}, & \delta > 0, \end{cases} \quad G(\delta) = \begin{cases} b + c\delta^2, & \delta \le 0 \\ b + \frac{\delta}{\delta_* - \delta}, & \delta > 0, \end{cases} \quad (10)$$

where b, c, d, ε and δ_* are model parameters specified in Table 1.

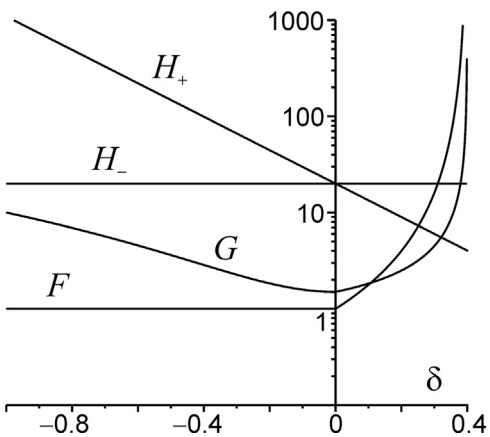

Fig. 1. The normalized rates of the crossbridge transitions between different crossbridge states *vs.* dimensionless ensemble-averaged crossbridge distortion, δ.

In Fig. 1 all normalized rate constants introduced above are shown as functions of the dimensionless distortion δ. To describe the mechanical properties of an activated muscle subjected to stretch, we assumed the rate of crossbridge binding to actin F to be an the increasing function of δ at positive δ. It was shown (Brunello et al., 2007) that stretch promotes binding of the second (partner) head of a myosin molecule to actin. As the two heads are connected with a common coiled-coil sub-fragment 2 of myosin, stretch of a head bound to actin probably brings its partner head to the position where it readily and quickly binds neighbour actin site of the same thin filament. A structural study (Ferenczi et al., 2014) have shown that during ramp stretch the vast majority of myosin heads is bound to actin in a non-stereospecific manner and they detach and reattach quickly like a pair of legs when muscle is subjected to lengthening. To simulate the fast binding of the second head and to describe the force-velocity curve during muscle elongation without explicit complicated consideration of two-headed crossbridges, we simply set the attachment and detachment rates to be increasing functions of the average crossbridge strain δ at positive δ.

2.3. Calcium activation

Contraction of striated muscle is regulated by Ca^{2+} ions which bind troponin-C (Tn) and enable myosin binding to actin. According to the 3-state model (McKillop and Geeves, 1993) in the absence of Ca^{2+} Tn binds actin and holds tropomyosin (Tpm) in the blocked state, or B-state, where it covers actin from myosin binding. Ca^{2+} binding to Tn releases Tpm which shifts to closed, or C-state, where myosin heads can bind actin. Transition of the actin-myosin bond from the weak and non-stereo-specific mode to the strong stereo-specific one shifts the Tpm strands further to the open, or O-state, where neighbour actin sites are available for myosin binding. Initial Ca^{2+} binding to Tn was shown to be very fast (> 1000 s^{-1}) and probably quickly reversible while the B- to C-state transition has the rate constant of ~100 s^{-1} (Fusi et al., 2014). To characterise the fraction of actin sites available for myosin binding, i.e., those in the C- or O-states in the filament overlap zone of sarcomere where myosin heads can bind actin and outside this zone, we use separate variables, A_1 and A_2, respectively. In the overlap zone strong stereo-specific binding of myosin heads to actin increases the Tn affinity for Ca^{2+} and keeps Tmp in the O-state. Recent data of Fusi et al. (2014), who have shown that Ca^{2+} binding to Tn itself is very fast, justify a more simple one-step kinetics of muscle activation by Ca^{2+} ions, as it was suggested by Izakov et al. (1991) and was further developed by Markhasin et al. (2003), compared to the two-step kinetic scheme used by Razumova et al. (2000), Niederer et al. (2006), Rice et al. (2008): Ca^{2+} binding to Tn followed by a Tpm transition from the B- to C-state. Indeed as Ca^{2+} binding itself is fast, one can assume it to be infinitely fast and to reduce the number of ODEs in the model.

In cardiac muscle Tn-C has only one binding site for Ca^{2+}. However there is high cooperativity in Ca^{2+} binding to Tn: even when strong binding of myosin heads to actin was blocked by blebbistatin the cooperativity Hill parameter for Ca^{2+} binding to Tn-C was ~3 (Sun et al., 2009; Sun and Irving, 2010). The reason for the cooperativity is probably the mechanical stiffness of Tpm and helical shape of the Tpm strand that results in long-range interaction of Ca^{2+} binding-unbinding to neighbour Tn molecules (Metalnikova, Tsaturyan, 2013). There is another type of cooperativity between Ca^{2+} binding to Tn-C and myosin binding to actin as well as the dependencies of both these processes on sarcomere length (Gordon et al., 2000). The last type of cooperativity called 'length depended activation' is the structural basis of the 'Starling law of the heart' (de Tombe et al., 2010).

The kinetic equations for A_1 and A_2 were then written in the form:

$$\frac{\partial(W(l_s)A_1)}{\partial t} = W(l_s)(\alpha_+(c(1-A_1)^{1/m} - a(l_s, n\theta)A_1^{1/m})) + \begin{cases} \frac{\partial W(l_s)}{\partial t}A_2, & \frac{\partial W(l_s)}{\partial t}>0, \\ \frac{\partial W(l_s)}{\partial t}A_1, & \frac{\partial W(l_s)}{\partial t}\le 0, \end{cases} \quad (9)$$

$$\frac{\partial((l_a - W(l_s))A_2)}{\partial t} = (l_a - W(l_s))(\alpha_+(c(1-A_1)^{1/m} - a(l_s,0)A_1^{1/m})) - \begin{cases} \frac{\partial W(l_s)}{\partial t}A_2, & \frac{\partial W(l_s)}{\partial t}>0, \\ \frac{\partial W(l_s)}{\partial t}A_1, & \frac{\partial W(l_s)}{\partial t}\le 0. \end{cases}$$

Here $c=C/C_0$ is normalized concentration of Ca^{2+} in muscle cell, where C is its concentration in μM and C_0 is characteristic value of C that corresponds to half-maximal Tn saturation at $l_s = l_{s0}$ in the absence of myosin heads; m is a constant that corresponds to the Hill parameter of the standard Hill approximation of the force-calcium relationship and accounts for the neighbour Tn interaction via elastic Tpm (Metalnikova, Tsaturyan, 2013), and α_+ is a characteristic rate constant of the Tpm transition to the C- and O-states upon Ca^{2+} binding to Tn; a depends on sarcomere length l_s to account for the length-dependent activation and on the fraction $n_2=n\theta$ of myosin heads which are strongly bound to actin in the overlap zone of sarcomere. The two first terms in the right hand side of Eq. (9) describe the forward and reverse transitions between the B- and C- and O-states, respectively. The last 'convective' terms in Eq. (9) proportional to $\frac{\partial W_a(l_s)}{\partial t}$ occur due to exchange between the overlap and non-overlap zone of a sarcomere upon its shortening or lengthening when Tn sites from the non-overlap zone move to the overlap zone or *vice versa*. The nonlinear kinetics used in Eq. (9) allows one to describe the cooperativity of the first type (the dependence of the Tpm transition from the B- to C-state and backwards on the state of neighbour Tmp molecules).

After identity transformations of the left and right sides of Eq. (9) we obtained the equations:

$$\frac{\partial A_1}{\partial t} = \alpha_+(c(1-A_1)^{1/m} - a(l_s, n\theta)A_1^{1/m}) + \begin{cases} 0, & \frac{\partial W(l_s)}{\partial t}\le 0, \\ \frac{\partial W(l_s)}{\partial t}\frac{(A_2 - A_1)}{W(l_s)}, & \frac{\partial W(l_s)}{\partial t}>0, \end{cases} \quad (9')$$

$$\frac{\partial A_2}{\partial t} = \alpha_+(c(1-A_2)^{1/m} - a(l_s,0)A_2^{1/m}) + \begin{cases} \frac{\partial W(l_s)}{\partial t}\frac{(A_2 - A_1)}{(l_s - W(l_s))}, & \frac{\partial W(l_s)}{\partial t}\le 0, \\ 0, & \frac{\partial W(l_s)}{\partial t}>0. \end{cases}$$

We used a in the form:

$$a(l_s, n\theta) = \frac{1}{(1+k_s(l_s - l_{s0})/l_{s0})(1+k_n n\theta)},$$

where k_s and k_n are constants. The first constant accounts for the length dependence of activation of cardiac muscle, while the second one describes the cooperativity of the second type (the dependence of activation on the fraction of strongly bound crossbridges).

It was found that apart from Tn there are some other Ca^{2+} buffers in the ventricular myocytes of mammals (Berlin et al., 1994). The buffers are fast, they have the total Ca^{2+} capacity of $B \approx 100$ μM and an effective equilibrium constant $K_B \approx 1$ μM. Assuming that calcium binding to the buffer is fast, we used the simplest calcium balance equations in the form:

$$\left(1+\frac{BK_B}{(c + K_B)^2}\right)\frac{\partial c}{\partial t} = Q(t) - \frac{\lambda(c - c_*)}{cK_i+1} - \frac{C_{Tn}}{l_a C_0}\frac{d(A_1 W(l_s) + A_2(l_a - W(l_s)))}{dt}, \quad (10)$$

where

$$Q(t) = Q^*(\exp(-k_1 t) - \exp(-k_2 t))$$

is the rate of Ca^{2+} inflow from sarcoplasmic reticulum and extracellular space; k_1, k_2, Q^*, c_* are constants; λ is the rate constant of Ca^{2+} uptake into sarcoplasmic reticulum and outside the cell; K_i is an equilibrium constant, C_{Tn} is the total molar concentration of Tn; c_* is the normalized Ca^{2+} concentration in relaxed muscle, and l_a is the length of an actin filaments. The model consists of Eqs. (8) or (8′) depending on the presence of fast perturbation in length or load, (9′) and (10), i.e. of 5 or 6 ODEs (see Appendix). These ODE system was solved numerically using a multistep Adams–Moulton method.

3. Results

3.1. Steady-state contraction at full activation and full filament overlap

The most reliable experiments of this type have been mainly performed with single intact muscle fibres of the frog under control of sarcomere length, although some data obtained from cardiac muscles were also reported. We compared the results of model simulation with experiments with intact fast muscle fibres using dimensionless normalized variables for further extension to other types of muscles including slow skeletal and cardiac ones. As in skeletal muscle passive tension is negligible compared to maximal active tension at full activation and full filament overlap, only active tension T_A is presented in figures below.

The steady-state force-velocity and stiffness-velocity relations for the model are shown in Fig. 2 together with the dependence of the fractions of actin-bound and force-generating myosin heads on the velocity of shortening or stretching.

The model force-velocity relation during steady shortening is very

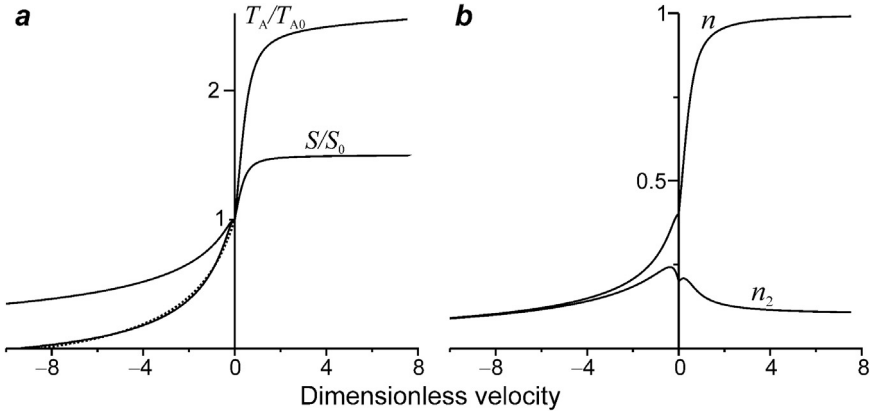

Fig. 2. a: continuous lines are simulated force-velocity and stiffness-velocity relationships. Stiffness S and active tension T_A normalized for their isometric values S_0 and $T_A°$ are plotted against normalized velocity of shortening (< 0) or stretch (> 0). Maximal dimensionless shortening velocity expressed in hf_+^0 units is 9.3 that correspond to 2.3 μm/s and 7.0 μm/s, for f_+^0 equal 25 s^{-1} and 75 s^{-1}, respectively. Dotted line is the Hill force-velocity relation with parameter a =0.26. b: simulated dependencies of the fractions of actin-bound, n, and force-generating, n_2, myosin heads on the dimensionless velocity.

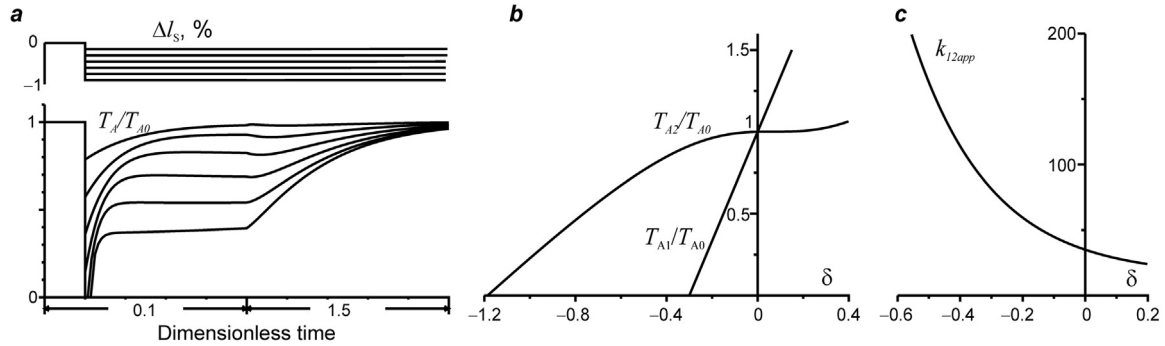

Fig. 3. Model simulations of tension responses to length step changes. a: bottom panel shows tension transients induced by step changes of different amplitudes shown in the upper panel, dimensionless time is expressed in $(1/f_+^0)$ units; b: tension immediately after the length step, T_{A1}, and at the end of the fast partial tension recovery (Huxley-Simmons phase 2), T_{A2}, normalized by isometric tension $T_A°$ plotted against the length step size per a half-sarcomere, Δl_s, normalized by the working stroke of the crossbridge, h; c: the apparent rate of the phase 2; c: k_{app}, *vs.* $\Delta l_s/h$ in reciprocal time units f_+^0.

close to that described by the Hill hyperbolic relation. Apparent half-sarcomere stiffness decreases with shortening velocity as was described by (Julian and Morgan, 1981; Ford et al., 1985). During stretch, active tension and instantaneous stiffness quickly increase and saturate at the levels above their isometric level (Fig. 2) as was found by Lombardi and Piazzesi (1990). The apparent instantaneous stiffness tightly correlates with the fraction of actin-bound heads. When muscle is stretched with a reasonably high velocity, a vast majority of the heads becomes bound to actin although very few of them are bound strongly and can generate force (Fig. 2). This model features also agree with experimental data showing that during ramp stretch a majority of the heads are bound to actin in a non-stereo-specific manner (Ferenczi et al., 2014) and do not consume much ATP (Bickham et al., 2011).

3.2. Mechanical transients caused by step changes in length or load

Simulated responses to fast changes in fibre length and load at full activation and full filament overlap are shown in Figs. 3 and 4. The results of simulation of the Huxley-Simmons transients (Huxley and Simmon, 1971; Ford et al., 1977) closely resemble experimental data (Fig. 3).

As was found experimentally (Ford et al., 1977) instantaneous muscle stiffness is Hookean while the fast partial tension recovery immediately after the step is nonlinear in its amplitude (Fig. 3b) and rate (Fig. 3c). After small amplitude shortening tension quickly recovers to a near isometric level, while for larger steps fast tension recovery in incomplete (Fig. 3b). The larger the shortening step the faster the partial tension recovery in phase 2 (Fig. 3c).

Another type of unsteady experiments with contracting muscle is monitoring of length changes induced by load step changes (Civan and Podolsky, 1966; Piazzesi et al., 2002). The results of simulation of this type of experiments are shown in Fig. 4.

The length changes following a step change in load have several phases: instantaneous drop during the load step itself, fast shortening at a constant load that corresponds to phase 2 of the Huxley-Simmons transients, slowing of the shortening or a plateau followed by steady state shortening at a constant velocity that corresponds to a point on the force-velocity diagram (Fig. 4). All these features as well as the fact that after large load changes the steady shortening begins earlier than after small ones are observed experimentally (Piazzesi et al., 2002).

3.3. Tension response to ramp stretches

The results of simulation of this type of experiments by the model are shown in Fig. 5.

As found by Lombardi and Piazzesi (1990) tension settling during stretch depends on velocity. For slow stretch tension achieves a steady level slowly and monotonically; at faster stretch there is an overshoot. The faster the stretch the faster tension achieves its steady-state level. All these features are reproduced by the model (Fig. 5).

3.4. Tension response to small-amplitude oscillations in fibre length

The results of model simulation of such experiments are shown in Fig. 6.

Our model reproduces the presence of a range of oscillation frequencies for which the imaginary part of stiffness is negative, or, in other words, muscle viscosity is apparently negative. This means that in this frequency range muscle produces positive work during a stretch-release cycle, in contrast to passive materials not producing active tension. This phenomenon was found for skeletal (Kawai et al., 1981) and cardiac (Saeki et al., 1991) muscles. For f_+^0=25 s^{-1} maximal work is produced at frequency of 16 Hz.

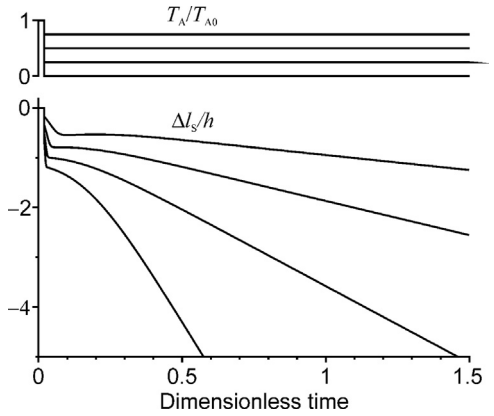

Fig. 4. The result of model simulation of length changes induced by load steps in muscle fibres. Upper tracers: changes in normalized tension; lower traces: changes in sarcomere length normalized by step size, h, *vs.* dimensionless (normalized) time in $(1/f_+^0)$ units.

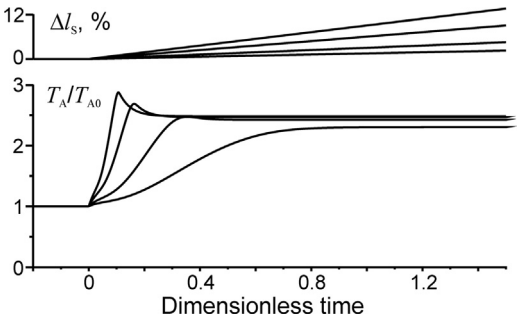

Fig. 5. Tension responses to ramp muscle stretch obtained from the model. Upper traces: changes in fibre length in %; lower traces: tension responses normalized by isometric tension. Time is expressed in $(1/f_+^0)$ units.

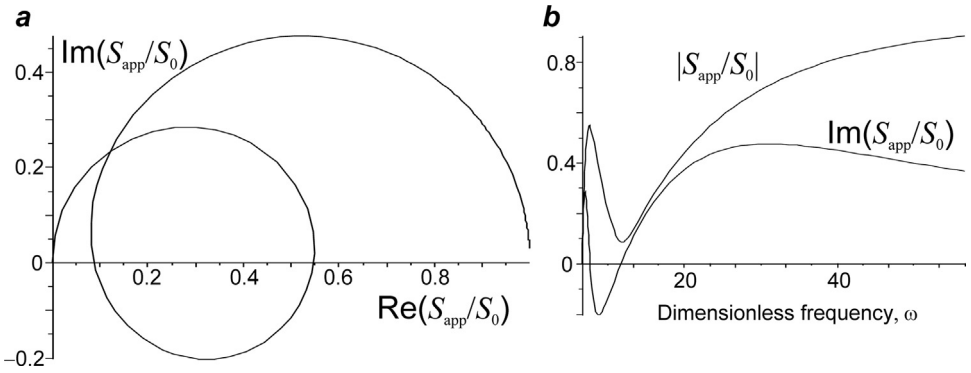

Fig. 6. Results of simulation of tension responses to small-amplitude oscillations of fibre length. a: Nyquist plot of imaginary and real parts of apparent fibre stiffness; b: the dependence of the amplitude and imaginary parts of stiffness on dimensionless oscillation angular frequency ω expressed in f_+^0 units.

3.5. Ca-tension diagrams at different sarcomere length

Steady state force-calcium curves at different constant sarcomere length characterize so called length dependent activation that is basis of the Starling law of the heart (de Tombe et al., 2010). Normalized tension calculated for our model at different constant sarcomere length is shown in Fig. 7.

Model calculations reproduce well experimental data (Dobesh et al., 2002). The A_1 dependence on calcium concentration in the absence of myosin heads is shifted to the right showing that actin-bound myosin heads increase Ca^{2+} sensitivity by 0.15 pCa units as it was found experimentally (Sun, Irving, 2010). The model describes a decrease in steepness of the diagram at higher force compared to the Hill equation found experimentally (Dobesh et al. (2002)). The model also reproduces a decrease in the Ca^{2+} concentration required for half-maximal activation by ~0.3 pCa units (Sun, Irving, 2010) caused by an inhibitor of strong actin-myosin binding, blebbistatin. However the decrease in steepness of the force-calcium diagram in the absence of myosin heads obtained with our model calculations (Fig. 7b) is somewhat more significant than observed experimentally.

3.6. Tension responses to Ca^{2+} jumps and force redevelopment

We also simulated the results of the experiments of Pirrodi et al. (2007) who studied properties of single myofibrils from human atrial and ventricural myocardium. To characterize the kinetics of Ca^{2+} activation and crossbridge attachment they have studied tension development upon fast increase in Ca^{2+} concentration and force redevelopment upon mechanical perturbation at different constant levels of Ca^{2+}. The results of simulation of their experimental protocol are shown in Fig. 8. At time zero, normalized Ca^{2+} concentration was increased quickly from a diastolic level to different constant values. When steady-state tension was achieved, the model myofibril was released by 10% of its length and then re-stretched to its initial length 20 ms later. The apparent rate constant of tension re-development k_{tr} was close to that of tension development upon Ca^{2+} activation, k_{ACT}, at all Ca^{2+} concentrations tested, and both rates increased with the increase in calcium concentrations and steady-state tension (Fig. 8) as it was found experimentally (Piroddi et al., 2007). At high Ca^{2+} concentration the rate constants were ~16 s^{-1}, i.e. about 15 times those measured by Piroddi et al. (2007) in myofibrils from human left ventricle at 15 °C. Taking into account that temperature coefficient Q_{10} for k_{tr} in cardiac muscle is ~3.5 (de Tombe and Stienen, 2007) our simulation provides reasonable values for both rate constants for human cardiac muscle at physiological temperature 37 °C.

3.7. Twitch contractions at different sarcomere length

The results of simulation of isometric twitch contractions at different constant sarcomere length by our model are shown in Fig. 9.

As was observed experimentally by ter Keurs (2012), an increase in sarcomere length led to a significant increase in the amplitude and

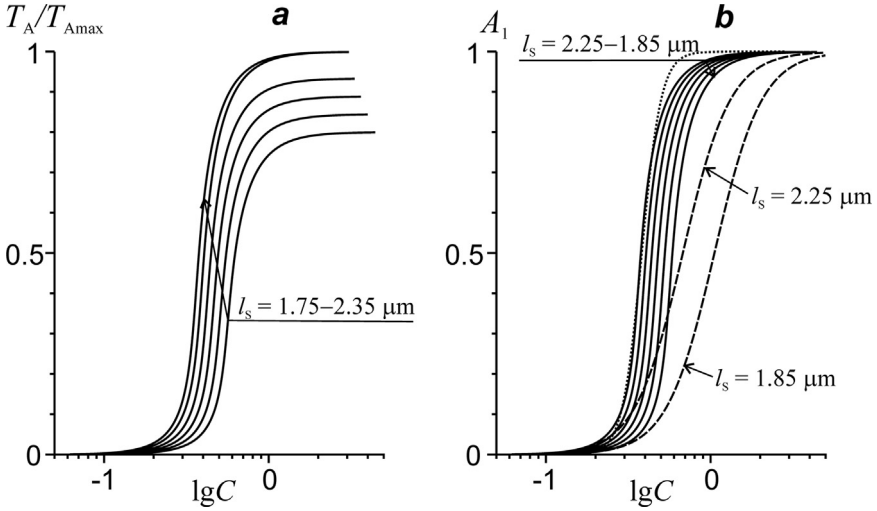

Fig. 7. Simulated calcium-force diagram: isometric tension *vs*. logarithm of normalized Ca^{2+} concentration (pCa) at different sarcomere length (shown next to the curves). a: active tension normalized by its maximal value at l_s =2.25 μm; b: the same curves normalized by maximal tension at C =10×C_0. Normalized activation A_1 (fraction of activated Tn-Tpm complexes in the overlap zone) at sarcomere length 1.85 and 2.25 μm in the absence of myosin heads (n =0) are shown by dashed lines. Dotted line is the fit of the normalized Ca-force diagram at l_s =2.25 μm with the Hill equation (cooperativity coefficient n =4.9, c_{50} =0.357).

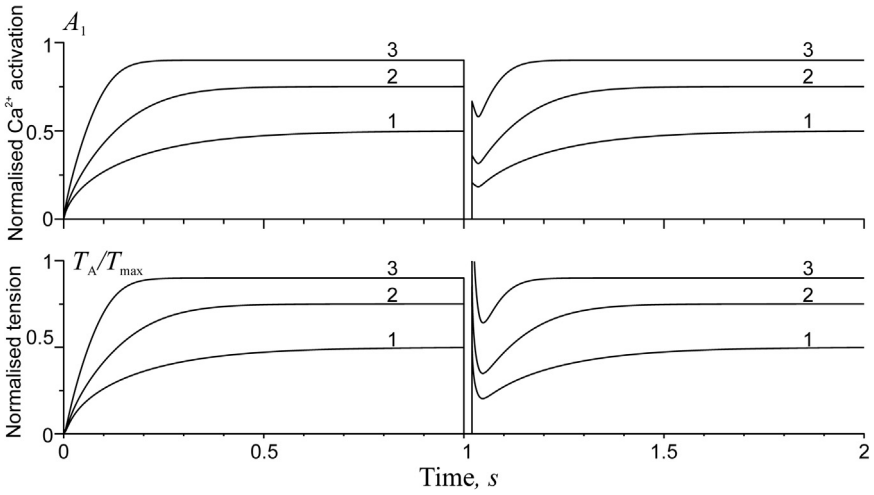

Fig. 8. Results of model simulation of tension transients induced by fast increase in Ca^{2+} concentrations and during force redevelopment caused by muscle release followed by re-stretch. The traces labelled 1, 2, and 3 correspond to the increase in normalized Ca^{2+} concentration from 0.05 to 0.46, 0.54 and 1.04, respectively. At time t=1 s muscle was released by 10% and re-stretched to its initial length at time 1.02 s. Upper panel shows the time course of thin filament activation in the overlap zone, A_1. Lower panel shows calculated transients of normalized active tension.

duration of isometric twitches in the model and also induced a deceleration of the early stages and a slowing down of the late stages of Ca^{2+} relaxation (Kentish and Wrzosek, 1998; ter Keurs, 2012). The difference between calculated degrees of Ca^{2+} saturation of Tn sites within overlap zone and outside it, A_1 and A_2, was quite significant (Fig. 9). This justifies the use of two different variables for these values in our model. Peak of calcium concentration was achieved earlier than that of tension while the decay of Ca^{2+} concentration was somewhat slower than tension relaxation, as it was observed by Kentish and Wrzosek (1998), ter Keurs (2012) and other authors and as it was obtained in model of Land and Niederer (2015) using a much more complicated and sophisticated model. The normalized peak Ca^{2+} concentration was higher than its diastolic level by a factor of 10 as was observed in cardiac muscle from different species (Land and Niederer, 2015).

3.8. Load-dependent relaxation in twitch contractions

The results of simulation of isotonic contractions in different types of contraction are shown in Fig. 10. In the first type of experiment, muscle contract isometrically until tension achieves certain pre-set load level. Then it shortens and relaxes under constant load until sarcomere length returns to its isometric level. Final relaxation is again isometric (Fig. 9a). For the second type, the switch from isotonic to isometric contraction occurs when muscle shortening stops. Then muscle relaxes under isometric conditions (Fig. 9b).

The model reproduces load dependent relaxation of cardiac muscle: the lower the load the shorter is isotonic contraction and the faster is subsequent isometric relaxation. Similar behaviour was observed experimentally in rat myocardium from the left (Capasso et al., 1989; Izakov et al., 1991), but neither from the right ventricle (Capasso et al., 1989) nor isolated frog myocytes (Parikh et al., 1993).

4. Discussion

4.1. Comparison with previous models

The idea of using ensemble averaged crossbridge strain, δ, instead of individual strain of each particular crossbridge, as it was initially suggested by Huxley (1957), goes back to work of Thorson and White (1983) who used this approach to simulate tension responses to small-amplitude length perturbations in skeletal and insect flight muscle. Later Razumova et al. (1999) suggested a model that used the Huxley-Simmons (1971) approximation of the kinetic scheme of myosin heads with three structurally different states. The scheme was then used by many researchers. Assuming that Huxley-Simmons force-generating transition is fast and reversible, we reduced the model and left over with only one variable, δ, that describes ensemble-averaged cross-bridge strain as was done by Thorson and White (1983). Moreover, for relatively slow processes the fraction of force-generating cross-bridges

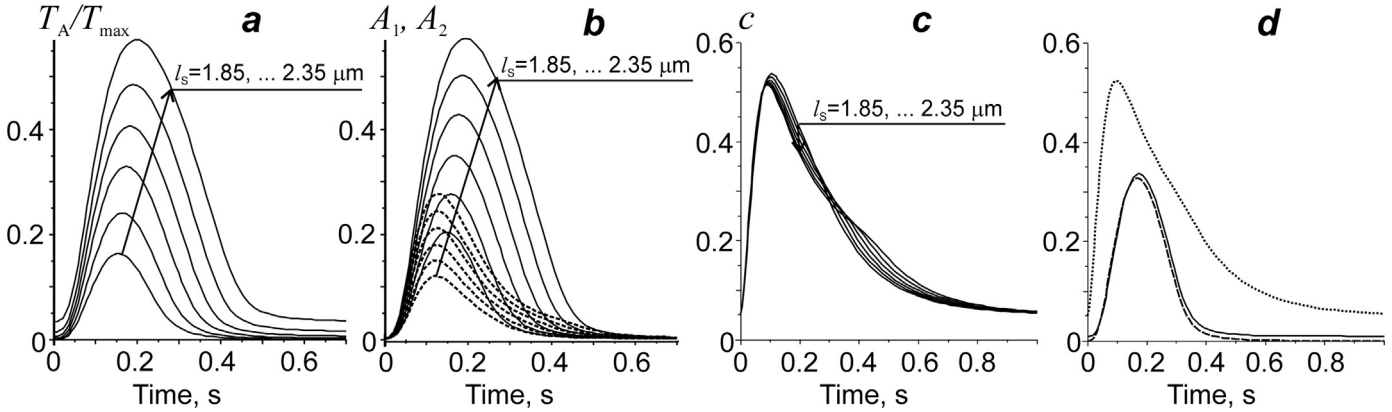

Fig. 9. Results of simulation of isometric twitch contractions at different sarcomere length (shown next to the curves). a: normalized tension; b: A_1 (continuous lines) and A_2 (dotted lines); c: normalized calcium concentration; d: calculated transients of normalized Ca^{2+} concentration (dotted line), A1 (dashed line) and normalized tension (continuous line) at sarcomere length 2.05 μm.

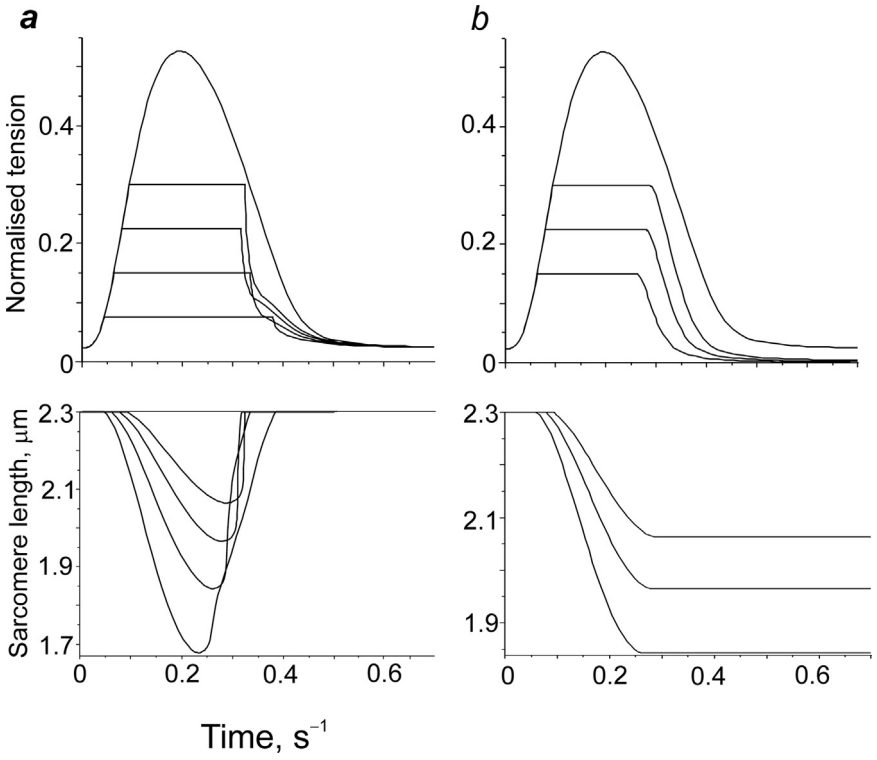

Fig. 10. Results of simulation of isotonic contractions in different modes. a: isotonic contraction at four levels of load with return to initial sarcomere length followed by isometric relaxation; b: isotonic contractions at different load, which were switched to isometric mode at the end of shortening. Upper traces are normalized tension, bottom ones show sarcomere length.

among all actin-attached ones, θ, becomes known function of δ and active force is determined by two variables only: δ and the fraction of actin-bound myosin heads, *n*. Both these simplifications make the ODE system less stiff and simpler computationally. Our model uses strain-dependent rate constants of crossbridge binding and detachment in order to account for large deformations.

In contrast to approach of Izakov et al. (1991) and Hunter et al. (1998) we do not postulate Hill force-velocity and stiffness-velocity relationships for steady-state contractions. These relationships were obtained as a result of a more general approach that accounts for strain-dependent rates of the transitions between the crossbridge states (Fig. 2). We also did not set up the time course of tension relaxation induced by a step length change as was done by Hunter et al. (1998) and Niederer et al. (2006). Instead mechanical responses to step perturbations in muscle length (Fig. 3) or force (Fig. 4) as well as tension responses to small-amplitude oscillation of muscle length (Fig. 6) resulted from the same strain-dependent crossbridge kinetics. We have previously shown that even an early version of this model (Syomin and Tsaturyan, 2012) is capable to describe tension responses to fast length changes applied during steady shortening (Ford et al., 1985) and lengthening (Piazzesi et al., 1992) as well as repriming of force generation observed in experiments with two subsequent length steps (Lombardi et al., 1992). The new version of the model presented here also explains tension transients caused by ramp stretch of fully activated muscle at full filament overlap (Fig. 5).

In contrast to models (Hunter et al., 1998; Razumova et al., 2000; Niederer et al., 2006; Rice et al., 2008) and similarly to models (Izakov et al., 1991; Markhasin et al., 2003) we assumed that Ca^{2+} binding to Tn is very fast and reversible while Tpm transitions from the B- to C- and O-state and *vice versa* are cooperative and occur at a slower time scale as found experimentally (Fusi et al., 2014). Assumption of two-step or more complicated kinetics of Ca^{2+} binding to Tn and Tpm transition from the B- to O-state leads to unnecessary complication of the model. In contrast to many previous models our approach also provides similar calcium dependencies for normalized tension and normalized concentration of Tn-Ca^{2+} complexes as was found experimentally (Sun et al., 2009). To account for the influence of actin-bound myosin heads on Ca^{2+} binding to Tn, we separately describe kinetics of Ca^{2+} binding to Tn in the filament overlap zone and outside it. In both zones the affinity of Tn for Ca^{2+} depends on sarcomere length while in the overlap zone it also depends on the fraction of force-generating myosin heads. Although Rice et al. (2008) also assumed the presence of two types of Ca^{2+} binding to Tn, our model is, to our knowledge, the first one where transition of Tn complexes from and to the overlap zone is accounted for explicitly. Non-linear kinetics of Ca^{2+} binding to Tn allowed us to account for Tn-Tn cooperative interaction and obtain reasonably steep calcium curves, while length-dependence of activation and its dependence on the fraction of force-generating myosin heads provided good approximation of the Starling law at the cellular level and the effect of blebbistatin on the force-calcium relationship (Fig. 7). The model describes the kinetics of myofibril activation induced by Ca2+ jump and tension redevelopment upon mechanical perturbation (Fig. 8). It also reproduces the time course of tension and of the fractions of the Tn-Tpm complexes in the C- and O-states and the free Ca^{2+} concentration in a cell during a twitch (Fig. 9). Moreover, the model reproduces the dependence of the of Ca^{2+} transients on sarcomere length that was observed experimentally (ter Keurs, 2012), although such dependence was not directly introduced into the model. Model also reproduced load dependent relaxation, i.e., acceleration of isometric relaxation after isotonic shortening at low load (Fig. 10). To our knowledge this is the first model that reproduces qualitatively all these experiments with a single set of parameters.

4.2. Choice of model parameters

The number of parameters that determine the actin-myosin interaction and its strain dependence is also fewer than in previous models of this type and our early model (Syomin and Tsaturyan, 2012). The model parameters which determine model behaviour at full activation were estimated as follows. Parameter b =1.5 provides the fraction of

actin-bound myosin heads during isometric contraction at full activation to be 0.4 as found experimentally (Tsaturyan et al., 2011). To obtain low muscle stiffness at maximal shortening velocity (Julian Morgan, 1981; Ford et al., 1985) we set c =8.5. The dependencies of muscle tension and stiffness on stretch velocity (Lombardi and Piazzesi, 1990) can be well described (Fig. 2) with δ^*= 0.4. Fast tension transient induced by step changes in ether length or load were well described with a Huxley-Simmons (1971) type model with parameters h =10 nm, H_-= 20 k_+^0 and γ=0.4. Filament compliance e was assumed to be 2 nm/T_0 where T_0 is isometric tension as estimated experimentally by Linari et al. (1998) and the time scaling rate constant k_+^0=75 s^{-1} was chosen to obtain maximal shortening velocity of 7 μm/s. All simulations of experiments with skeletal muscle fibres at full activation shown in Figs. 2–6 were performed with the same set of parameters.

The values of parameters which determine Ca^{2+}-activation in our model were estimated as follows. To obtain reasonably high Hill coefficient, we set m =3. Coefficients which characterise length-dependent activation, k_s, was chosen to fit experimental data of Dobesh et al. (2002). Parameter k_n which characterises an increase in the Tn affinity for Ca^{2+} upon binding of myosin heads to actin was estimated as follows. Full saturation of reconstructed thin filaments with rigor myosin heads increases Tn affinity for Ca^{2+} by a factor of 8 (Sun et al., 2009). We, therefore, set k_n =8. With this value our model was able to describe changes in the Ca^{2+} curves in permeabilized cardiac muscle caused by blocking strong binding of myosin heads to actin with blebbistatin (Sun and Irving, 2010). Values of the total Tn concentration in cardiac muscle cell and the characteristic half-saturation Ca^{2+} concentration were taken from available data. The only time constant that characterises the kinetic of muscle activation is α_+. The rate of Tmp transition from the B- to C or O-state was measurement only in fast skeletal muscle of the rabbit by Fusi et al. (2014) who estimated the sum of the forward and backward rate constants to be ~120 s^{-1} at 12°C. In the absence of direct measurements of this value for cardiac muscle we estimated α_+ from the positions of the peaks of Ca^{2+} transient and tension. A ~0.1 s delay between the peaks can be reproduced with α_+= 35 s^{-1}. Apart from parameters listed above, tuning of our model for simulation of contractions of cardiac muscle from particular species at certain temperature would include adjustment of model parameters which determine Ca^{2+} release from terminal cisterns of SR, and currents via L-channels and NaCa exchange as well as Ca^{2+} uptake into SR.

5. Conclusion

Despite its simplicity, our model qualitatively reproduces all experimentally observed phenomena listed in the Introduction section and is quite effective computationally as the only “fast” variable θ can be omitted if one considers only relatively slow contraction and relaxation processes with the characteristic time of 2–3 ms or longer. The model describes a number of different experiments with cardiac muscle by a few ODEs with a limited set of parameters. We believe that the model can be useful for multi-scale simulation of heart mechanics.

Acknowledgements

The work was supported by grant 14-35-00005 from the Russian Science Foundation (RSF).

Appendix

Full set of model equations

Constitutive equation which determines Cauchy stress tension $\hat{T}$:

$$\hat{T} = \left(\frac{\partial\Phi(I_1, I_2)}{\partial I_1} + I_1\frac{\partial\Phi(I_1, I_2)}{\partial I_2}\right)\hat{F} - \frac{\partial\Phi(I_1, I_2)}{\partial I_2}\hat{F}^2 - p\hat{E} + \hat{B}(T_{tit} + T_A), \tag{A1}$$

where Φ is the isotropic strain energy function; F, I_1 and I_2 are the left Cauchy–Green deformation tensor and its first and second invariant, T_{tit} is anisotropic titin tension that contributes to passive myocardial force and is aligned with muscle fibres. Active tension T_A that also is also aligned with fibres is determined by expression:

$$T_A = EN_M N_{xb} W(l_s) hn(\delta + \theta), \tag{A2}$$

where E, N_M, N_{xb} are constants, W is the length of the overlap zone between the thin and thick filaments that depend on sarcomere length l_s. Variable n, δ and θ are the fraction of actin-bound crossbridges in the overlap zone, ensemble average strain of crossbridges normalized by the step size h, and the fraction of force-generating crossbridges among the actin-bound ones, respectively. The crossbridge binding and detachment are described by kinetic equation:

$$\frac{\partial n}{\partial t} = F(\delta)(A_1 - n) - nG(\delta), \tag{A3}$$

where F and G are the binding and detachment rates and A_1 is the fraction of the regulatory units in the C- or O-states in the overlap zone.

The changes in δ and θ in the full model are described by equations:

$$\frac{\partial\delta}{\partial t} = \frac{1}{2h}\frac{\partial l_s}{\partial t} - \frac{e}{h}\frac{\partial T_A}{\partial t} - \delta F\frac{(A_1 - n)}{n}, \tag{A4}$$

$$\frac{\partial\theta}{\partial\tau} = \frac{\theta_0(\delta) - \theta}{1 + \exp(-\alpha\delta)}, \quad \tau = \frac{t}{\varepsilon}, \tag{A5}$$

where e is compliance of the thin and thick filaments and $\theta_0(\delta)$ is known function

For relatively slow processes which last more than 2–3 ms, a reduced model with simplified equations for δ and θ can be used to simplify calculations:

$$\frac{\partial\delta}{\partial t} = \frac{1}{2h}\frac{\partial l_s}{\partial t} - \delta F\frac{(A_1 - n)}{n}, \tag{A4′}$$

$$\theta = \theta_0(\delta). \tag{A5'}$$

Normalized occupancies of the C- and O-states in the overlap zone, A_1, and of the C-state outside this zone, A_2, are described by equations:

$$\frac{\partial A_1}{\partial t} = \alpha_+(c(1-A_1)^{1/m} - a(l_s, n\theta){A_1}^{1/m}) + \begin{cases} 0, & \frac{\partial W(l_s)}{\partial t} \le 0, \\ \frac{\partial W(l_s)}{\partial t}\frac{(A_2 - A_1)}{W(l_s)}, & \frac{\partial W(l_s)}{\partial t} > 0, \end{cases} \tag{A6}$$

$$\frac{\partial A_2}{\partial t} = \alpha_+(c(1-A_2)^{1/m} - a(l_s,0){A_2}^{1/m}) + \begin{cases} \frac{\partial W(l_s)}{\partial t}\frac{(A_2 - A_1)}{(l_s - W(l_s))}, & \frac{\partial W(l_s)}{\partial t} \le 0, \\ 0, & \frac{\partial W(l_s)}{\partial t} > 0. \end{cases} \tag{A7}$$

Normalized calcium concentration, c, obeys the equation

$$\left(1+\frac{BK_B}{(c + K_B)^2}\right)\frac{\partial c}{\partial t} = Q(t) - \frac{\lambda(c - c_*)}{cK_i+1} - \frac{C_{Tn}}{l_a C_0}\frac{d(A_1 W(l_s) + A_2(l_a - W(l_s)))}{dt}, \tag{A8}$$

where $Q(t)$ is calcium release assumed to be a given function of time, B, K_B, c_*, λ, K_i, C_0, C_{Tn}.

The meaning of all variables and values of the model parameter are given in Table 1.

References

Bershitsky, S.Y., Tsaturyan, A.K., 1981. Nature of muscular tissue anisotropy. Dokl. Akad. Nauk SSSR (Sov. Phys. Dokl.). 259, 53–56.

Berlin, J.R., Bassani, J.W., Bers, D.M., 1994. Intrinsic cytosolic calcium buffering properties of single rat cardiac myocytes. Biophys. J. 67, 1775–1787.

Bickham, D.C., West, T.G., Webb, M.R., Woledge, R.C., Curtin, N.A., Ferenczi, M.A., 2011. Millisecond-scale biochemical response to change in strain. Biophys. J. 101, 2445–2454.

Brunello, E., Reconditi, M., Elangovan, R., Linari, M., Sun, Y.B., Narayanan, T., Panine, P., Piazzesi, G., Irving, M., Lombardi, V., 2007. Skeletal muscle resists stretch by rapid binding of the second motor domain of myosin to actin. In: Proceedings Natl. Acad. Sci. USA., 104, pp. 20114–20119.

Capasso, J.M., Puntillo, E., Olivetti, G., Anversa, P., 1989. Differences in load dependence of relaxation between the left and right ventricular myocardium as a function of age in rats. Circ. Res. 65, 1499–1507.

Chiu, Y.L., Ballou, E.W., Ford, L.E., 1982. Velocity transients and viscoelastic resistance to active shortening in cat papillary muscle. Biophys. J. 40, 121–128.

Chiu, Y.C., Ballou, E.W., Ford, L.E., 1987. Force, velocity, and power changes during normal and potentiated contractions of cat papillary muscle. Circ. Res. 60, 446–458.

Civan, M.M., Podolsky, R.J., 1966. Contraction kinetics of striated muscle fibres following quick changes in load. J. Physiol. 184, 511–534.

Colomo, F., Poggesi, C., Tesi, C., 1994. Force responses to rapid length changes in single intact cells from frog heart. J. Physiol. 475, 347–350.

Dobesh, D.P., Konhilas, J.P., de Tombe, P.P., 2002. Cooperative activation in cardiac muscle: impact of sarcomere length. Am. J. Physiol. Heart Circ. Physiol. 282, H1055–H1062.

Ferenczi, M.A., Bershitsky, S.Y., Koubassova, N.A., Kopylova, G.V., Fernandez, M., Narayanan, T., Tsaturyan, A.K., 2014. Why muscle is an efficient shock absorber. PLoS One 9, e85739. http://dx.doi.org/10.1371/journal.pone.0085739, (eCollection 2014).

Ford, L.E., Huxley, A.F., Simmons, R.M., 1977. Tension responses to sudden length change in stimulated frog muscle fibres near slack length. J. Physiol. 269, 441–515.

Ford, L.E., Huxley, A.F., Simmons, R.M., 1985. Tension transients during steady shortening of frog muscle fibres. J. Physiol. 361, 131–150.

Ford, L.E., Huxley, A.F., Simmons, R.M., 1986. Tension transients during the rise of tetanic tension in frog muscle fibres. J. Physiol. 372, 595–609.

Fusi, L., Brunello, E., Sevrieva, I.R., Sun, Y.B., Irving, M., 2014. Structural dynamics of troponin during activation of skeletal muscle. In: Proceedings Natl. Acad. Sci. USA. 111. 4626–4631.

Gordon, A.M., Homsher, E., Regnier, M., 2000. Regulation of contraction in striated muscle. Physiol. Rev. 80 (2), 853–924.

Guccione, J.M., McCulloch, A.D., Waldman, L.K., 1991. Passive material properties of intact ventricular myocardium determined from a cylindrical model. J. Biomech. 113 (1), 42–55.

The heat of shortening and the dynamic constants of muscle. Proc. R. Soc. Lond. 126, 136–195.

Hunter, P.J., McCulloch, A.D., ter Keurs, H.E., 1998. Modelling the mechanical properties of cardiac muscle. Prog. Biophys. Mol. Biol. 69, 289–331.

Huxley, A.F., 1957. Muscle structure and theories of contraction. Prog. Biophys. Biophys. Chem. 7, 255–318.

Huxley, A.F., Simmons, R.M., 1971. Proposed mechanism of force generation in striated muscle. Nature 233, 533–538.

Izakov, V.Y., Katsnelson, L.B., Blyakhman, F.A., Markhasin, V.S., Shklyar, T.F., 1991. Cooperative effects due to calcium binding by troponin and their consequences for contraction and relaxation of cardiac muscle under various conditions of mechanical loading. Circ. Res. 69, 1171–1184.

Julian, F.J., Morgan, D.L., 1981. Variation of muscle stiffness with tension during tension transients and constant velocity shortening in the frog. J. Physiol. 319, 193–203.

Kawai, M., Cox, R.N., Brandt, P.W., 1981. Effect of Ca ion concentration on cross-bridge kinetics in rabbit psoas fibers. Evidence for the presence of two Ca-activated states of thin filament. Biophys. J. 135, 375–384.

Kentish, J.C., Wrzosek, A., 1998. Changes in force and cytosolic Ca^{2+} concentration after length changes in isolated rat ventricular trabeculae. J. Physiol. 506, 431–444.

Land, S., Niederer, S.A., 2015. A spatially detailed model of isometric contraction based on competitive binding of troponin I Explains Cooperative Interactions between Tropomyosin and Crossbridges. PLoS Comput. Biol. 11 (8), e1004376.

Leake, M.C., Wilson, D., Gautel, M., Simmons, R.M., 2004. The elasticity of single titin molecules using a two-bead optical tweezers assay. Biophys. J. 87, 1112–1135.

Linari, M., Dobbie, I., Reconditi, M., Koubassova, N., Irving, M., Piazzesi, G., Lombardi, V., 1998. The stiffness of skeletal muscle in isometric contraction and rigor: the fraction of myosin heads bound to actin. Biophys. J. 74, 2459–2473.

Liversage, A.D., Holmes, D., Knight, P.J., Tskhovrebova, L., Trinick, J., 2001. Titin and the sarcomere symmetry paradox. J. Mol. Biol. 305, 401–409.

Lombardi, V., Piazzesi, G., 1990. The contractile response during steady lengthening of stimulated frog muscle fibres. J. Physiol. 431, 141–171.

Lombardi, V., Piazzesi, G., Linari, M., 1992. Rapid regeneration of the actin-myosin power stroke in contracting muscle. Nature 355, 638–641.

Lombardi, V., Piazzesi, G., Ferenczi, M.A., Thirlwell, H., Dobbie, I., Irving, M., 1995. Elastic distortion of myosin heads and repriming of the working stroke in muscle. Nature 374, 553–555.

Lurie, A.I., 1990. Nonlinear Theory of Elasticity. Elsivier, Amsterdsm.

Lymn, R.W., Taylor, E.W., 1971. Mechanism of adenosine triphosphate hydrolysis by actomyosin. Biochemistry 10, 4617–4624.

Markhasin, V.S., Solovyova, O., Katsnelson, L.B., Protsenko, Yu, Kohl, P., Noble, D., 2003. Mechano-electric interactions in heterogeneous myocardium: development of fundamental experimental and theoretical models. Prog. Biophys. Mol. Boil. 82, 207–220.

Marko, J.F., Siggia, E.D., 1995. Stretching DNA Macromol. 28, 8759–8770.

Martyn, D.A., Gordon, A.M., 2001. Influence of length on force and activation-dependent changes in troponin C structure in skinned cardiac and fast skeletal muscle. Biophys. J. 80, 2798–2808.

McKillop, D.F., Geeves, M.A., 1993. Regulation of the interaction between actin and myosin subfragment 1: evidence for three states of the thin filament. Biophys. J. 65, 693–701.

Metalnikova, N.A., Tsaturyan, A.K., 2013. A mechanistic model of Ca regulation of thin filaments in cardiac muscle. Biophys. J. 105, 941–950.

Niederer, S.A., Hunter, P.J., Smith, N.P., 2006. A quantitative analysis of cardiac myocyte relaxation: a simulation study. Biophys. J. 90, 1697–1722.

Parikh, S.S., Zou, S.Z., Tung, L., 1993. Contraction and relaxation of isolated cardiac myocytes of the frog under varying mechanical loads. Circ. Res. 72, 297–311.

Piazzesi, G., Francini, F., Linari, M., Lombardi, V., 1992. Tension transients during steady lengthening of tetanized muscle fibres of the frog. J. Physiol. 445, 659–711.

Piazzesi, G., Lucii, L., Lombardi, V., 2002. The size and the speed of the working stroke of muscle myosin and its dependence on the force. J. Physiol. 545, 145–151.

Piroddi, N., Belus, A., Scellini, B., Tesi, C., Giunti, G., Cerbai, E., Mugelli, A., Poggesi, C., 2007. Tension generation and relaxation in single myofibrils from human atrial and ventricular myocardium. Pflug. Arch. 454, 63–73.

Razumova, M.V., Bukatina, A.E., Campbell, K.B., 1999. Stiffness-distortion sarcomere model for muscle simulation. J. Appl. Physiol. 87, 1861–1876.

Razumova, M.V., Bukatina, A.E., Campbell, K.B., 2000. Different myofilament nearest-neighbor interactions have distinctive effects on contractile behavior. Biophys. J. 78, 3120–3137.

Rice, J.J., Wang, F., Bers, D.M., de Tombe, P.P., 2008. Approximate model of cooperative activation and crossbridge cycling in cardiac muscle using ordinary differential equations. Biophys. J. 95, 2368–2390.

Saeki, Y., Kawai, M., Zhao, Y., 1991. Comparison of crossbridge dynamics between intact and skinned myocardium from ferret right ventricles. Circ. Res. 68, 772–781.

Smith, D.A., Geeves, M.A., Sleep, J., Mijailovich, S.M., 2008. Towards a unified theory of muscle contraction. I: foundations. Ann. Biomed. Eng. 36 (10), 1624–1640.

Sun, Y.B., Lou, F., Irving, M., 2009a. Calcium- and myosin-dependent changes in troponin structure during activation of heart muscle. J. Physiol. 587, 155–163.
Sun, Y.B., Irving, M., 2010. The molecular basis of the steep force-calcium relation in heart muscle. J. Mol. Cell Cardiol. 48, 859–865.
Syomin, F.A., Tsaturyan, A.K., 2012. A simple kinetic model of contraction of striated muscle: full activation at full filament overlap in sarcomeres. Biophysics 57, 840–847.
Syomin, F.A., 2014. A simple kinetic model of myocardium contraction: calcium-mechanics coupling. Biophysics 59, 951–958.
Thorson, J., White, D.C., 1983. Role of cross-bridge distortion in the small-signal mechanical dynamics of insect and rabbit striated muscle. J. Physiol. 343, 59–84.
Ter Keurs, H.E., 2012. The interaction of Ca^{2+} with sarcomeric proteins: role in function and dysfunction of the heart. Am. J. Physiol. Heart Circ. Physiol. 302 (1), H38–H50.
de Tombe, P.P., Mateja, R.D., Tachampa, K., Ait Mou, Y., Farman, G.P., Irving, T.C., 2010. Myofilament length dependent activation. J. Mol. Cell. Cardiol. 48, 851–858.
de Tombe, P.P., Stienen, G.J., 2007. Impact of temperature on cross-bridge cycling kinetics in rat myocardium. J. Physiol. 584, 591–600.
Trayanova, N.A., Rice, J.J., 2011. Cardiac electromechanical models: from cell to organ. Front Physiol. 2, 43. http://dx.doi.org/10.3389/fphys.2011.00043, (eCollection 2011).
Tsaturyan, A.K., Bershitsky, S.Y., Koubassova, N.A., Fernandez, M., Narayanan, T., Ferenczi, M.A., 2011. The fraction of myosin motors that participate in isometric contraction of rabbit muscle fibers at near-physiological temperature. Biophys. J. 101, 404–410.